Journal of Computational Physics **148,** 416–432 (1999)
Article ID jcph.1998.6123, available online at http://www.idealibrary.com on IDEAL®

Relaxation Scheme for a Lattice–Boltzmann-type Discrete Velocity Model and Numerical Navier–Stokes Limit

Axel Klar

Fachbereich Mathematik und Informatik, Freie Universität Berlin, 14195 Berlin, Germany
E-mail: klar@math.fu-berlin.de

Received April 30, 1998; revised September 28, 1998

A discrete velocity model based on a lattice–Boltzmann approximation is considered in the low Mach number limit. A numerical scheme for this model working uniformly in the incompressible Navier–Stokes limit is constructed. The scheme is induced by the asymptotic analysis of the Navier–Stokes limit and works uniformly for all ranges of mean free paths. In the limit the scheme reduces to an explicit finite difference scheme for the incompressible Navier–Stokes equation, the Chorin projection method with MAC grid. Numerical results are presented and the uniform convergence of the scheme is established numerically. © 1999 Academic Press

Key Words: discrete velocity models; lattice–Boltzmann method; asymptotic analysis; low Mach number limit; incompressible Navier–Stokes equations; projection scheme; MAC grid; numerical methods for stiff equations.

1. INTRODUCTION

Lattice–Boltzmann methods are based on discrete velocity models of kinetic equations. In these methods the discrete velocity model is usually solved by an explicit discretization on a grid conforming with the discrete velocity vectors. In the limit for small Knudsen and Mach numbers an approximation of the incompressible Navier–Stokes equations is obtained. See [3, 10] for reviews on lattice–Boltzmann methods and [19] for a review on discrete velocity models. Numerous work on lattice–Boltzmann methods has been done in the last years, we refer to the references in the above-cited reviews and, e.g., to [1, 7, 20]. For connections to kinetic schemes we refer to [14].

However, in principle any kind of method or grid structure could be used to solve the discrete velocity model. This has already been mentioned in [5]. In particular, since the lattice–Boltzmann discretization is an explicit one, it does not take into account properly the stiffness of the equations in the limit of small Knudsen or Mach numbers. A very

0021-9991/99 $30.00

fine space and time discretization has to be used to obtain an approximation of the Navier–Stokes equations. This is reasonable in a variety of situations, for example, if flow in complex geometries is simulated. In this case the fine grid is not only a requirement needed by the method in general, but also a requirement due to the geometry. However, if it is desirable to use larger time and space discretizations, implicit discretizations have to be used. Such an approach has been used successfully for a large number of kinetic equations with stiff relaxation terms in fluid dynamic or diffusive limits and did lead to the development of asymptotic preserving methods; see [4, 13, 11, 12, 17, 15, 16].

The purpose of the present paper is to suggest an implicit time discretization working uniformly without the necessity to adapt time and space discretization to the smallness of the Knudsen and Mach number. In the limit for small Mach numbers the scheme tends to a standard projection scheme with staggered grid for the incompressible Navier–Stokes equations as in [8, 18, 21]. Section 2 contains a description of the results of the asymptotic procedure to obtain the incompressible Navier–Stokes equations from kinetic equations. Section 3 contains a lattice–Boltzmann-type discrete velocity model and its associated closed moment system. In Section 4 the time discretization of the numerical scheme for the discrete velocity model is considered. Section 5 considers the low Mach number limit leading to the projection method for the incompressible Navier–Stokes equations. Section 6 shows how the space discretization is done. Finally, Section 7 contains a numerical investigation of the scheme.

2. KINETIC EQUATIONS AND THE INCOMPRESSIBLE NAVIER–STOKES EQUATIONS

This section contains a short description of the incompressible Navier–Stokes limit of kinetic equations; see [2] for details. We consider equations of the form

$$\partial_t F + v \cdot \nabla_x F = C(F), \tag{1}$$

where $F = F(x, v, t)$ with $x \in D \in \mathbb{R}^d$, $d = 1, 2, 3$, $v = (v_1, v_2, v_3) \in \mathbb{R}^3$, $t \in [0, \infty)$. $C(F)$ denotes the collision operator. The invariants of the collision operator are assumed to be the collision invariants 1, v, $|v|^2$. An example is given by the Boltzmann collision operator; see, e.g. [6].

Introducing the diffusive space-time scaling $x \to x/\epsilon$ and $t \to t/\epsilon^2$, where ϵ is the mean free path, one obtains the scaled equation

$$\partial_t F + \frac{1}{\epsilon} v \cdot \nabla_x F = \frac{1}{\epsilon^2} C(F). \tag{2}$$

With the standard perturbation procedure (see, e.g. [2, 9]) the limit equation for (2) as ϵ tends to 0 is derived in the following way: Solutions of (2) are sought in the form

$$F = M(1 + \epsilon f),$$

where M is the normalized Maxwellian with zero drift,

$$M(v) = \frac{1}{(2\pi)^{3/2}} \exp\left(-\frac{|v|^2}{2}\right).$$

This represents the low Mach number limit. Using this ansatz in Eq. (1) yields

$$\epsilon^2 \partial_t f + \epsilon v \cdot \nabla_x f = Lf + \epsilon Q(f, f) + O(\epsilon^2), \tag{3}$$

where L denotes the linearized collision operator

$$Lg = M^{-1} DC(M) Mg$$

and Q is given by the second Frechet derivative of C around M:

$$Q(g, g) = \frac{1}{2} M^{-1} D^2 C(M)(Mg \vee Mg).$$

We define the projection onto the space of collision invariants,

$$Pf = \langle f \rangle + v \cdot \langle vf \rangle + \left\langle \frac{|v|^2 - 3}{3} f \right\rangle \frac{|v|^2 - 3}{2}, \tag{4}$$

where

$$\langle f \rangle = \int_{\mathbb{R}^3} f(v) M(v)\, dv.$$

An example which will be used in the following is the BGK collision operator,

$$C(F)(v) = -\frac{1}{\tau}(F(v) - M_F(v)), \tag{5}$$

where M_F is the Maxwellian function having moments with respect to 1, v, $|v|^2$ which are equal to those of F. This yields

$$L(f)(v) = -\frac{1}{\tau}(f - Pf)(v).$$

Writing f as

$$f = f_0 + \epsilon f_1 + \epsilon^2 f_2 + \cdots,$$

inserting this into Eq. (3), and collecting terms of equal power in ϵ gives equations for $f_0, f_1, f_2, \ldots$. The solvability conditions for these equations yield the form

$$f_0 = \rho_0 + v \cdot u_0 + \frac{|v|^2 - 3}{2} T_0,$$

where u_0 solves the incompressible Navier–Stokes equations:

$$\begin{aligned} \partial_t u_0 + u_0 \cdot \nabla_x u_0 + \nabla_x p &= \mu \Delta_x u_0 \\ \nabla_x \cdot u_0 &= 0 \end{aligned} \tag{6}$$

with pressure p. T_0 and ρ_0 are determined by a heat transfer equation and the Boussinesq relation (see [2]).

The viscosity coefficient μ is determined by the linearized collision operator L and has been computed, for example, in [2]. A simple example is again given by the BGK model, where $\mu = \tau$.

We note that for the derivation of the incompressible Navier–Stokes equations the moments of the distribution function with respect to

$$A(v) = \frac{1}{2}(|v|^2 - 5)v, \quad B(v) = v \otimes v - \frac{1}{3}|v|^2 I$$

are important in addition to the first five moments with respect to $1, v, |v|^2$ (see again [2]).

The boundary conditions for Eq. (3) are given by

$$|v \cdot n| f(x, v, t) = \int_{v' \cdot n > 0} R^x(v, v') f(x, v', t) M(v') |v' \cdot n| \, dv' \tag{7}$$

for $x \in \partial D$ and $v \cdot n < 0$. Here n is the outer unit normal at $x \in \partial D$. In particular, R^x has to fulfill

$$\int_{v \cdot n < 0} R^x(v, v') M(v) \, dv = 1. \tag{8}$$

This guarantees that there is no flux through the boundary:

$$\int_{v \cdot n < 0} |v \cdot n| f(x, v, t) M(v) \, dv = \int_{v \cdot n > 0} |v \cdot n| f(x, v, t) M(v) \, dv. \tag{9}$$

Thus, the total density in D is conserved. Extensions of the following to other boundary conditions, as, e.g., in- and outflow boundary conditions, are possible. Moreover, initial conditions have to be imposed.

3. A LATTICE–BOLTZMANN-TYPE DISCRETE VELOCITY MODEL AND THE ASSOCIATED MOMENT SYSTEM

We consider the simplest discrete velocity model in two dimensions leading in the small Mach number limit to the incompressible Navier–Stokes equation. It is chosen as in lattice–Boltzmann BGK methods with six velocities on a hexagonal grid. The following can be easily extended to more complicated models, like seven velocity models, including a rest particle, or nine velocity models on a square lattice.

The discrete velocities are given by

$$c_i = \left(c_i^{(1)}, c_i^{(2)}\right) = (\cos(\pi(i-1)/3), \sin(\pi(i-1)/3)), \quad i = 1, \ldots, 6, \tag{10}$$

and the occupation numbers by $N = (N_1, \ldots, N_6)$. The discrete velocity model is given by

$$\partial_t N_i + \partial_x c_i^{(1)} N_i + \partial_y c_i^{(2)} N_i = J^i(N) \tag{11}$$

with

$$J^i(N) = -\frac{1}{\tau}\left(N_i - N_i^{eq}\right). \tag{12}$$

The equilibrium distribution function is

$$N_i^{eq} = \frac{\rho}{6} + \frac{1}{3}\left(c_i^{(1)}u_1 + c_i^{(2)}u_2\right) + \frac{2}{3}\sum_{k,l}\left(c_i^{(k)}c_i^{(l)} - \frac{1}{2}\delta_{k,l}\right)u_k u_l \tag{13}$$

with the density

$$\rho = \sum_{i=1}^{6} N_i \tag{14}$$

and

$$u_k = \sum_{i=1}^{6} c_i^{(k)} N_i, \quad k = 1, 2. \tag{15}$$

We mention that u denotes here the momentum vector and not the velocity as in the usual lattice–Boltzmann notation. This simplifies slightly the statement of the following. The form of the collision operator is similar to the standard form used in six or seven velocity models in LB simulations (see, e.g., [20, 7]). See [1] for a derivation of two-dimensional LB models from a continuous model with a BGK collision operator as in (5).

In the following our aim is to transform Eqs. (11) into an equivalent system of moment equations for which it is more obvious how the numerical treatment has to be done. We consider three second-order moments,

$$v = \sum_{i=1}^{6}\left(\left(c_i^{(1)}\right)^2 - \frac{|c_i|^2}{2}\right)N_i = \sum_{i=1}^{6}\left(\left(c_i^{(1)}\right)^2 - \frac{1}{2}\right)N_i, \tag{16}$$

$$w = \sum_{i=1}^{6} c_i^{(1)}c_i^{(2)}N_i, \tag{17}$$

$$p = \theta - \frac{|u|^2}{2}, \tag{18}$$

where θ is defined by

$$\theta = \sum_{i=1}^{6}\frac{|c_i|^2}{2}N_i - \frac{C}{2} = \frac{1}{2}\left(\sum_{i=1}^{6} N_i - C\right), \tag{19}$$

C a constant defined later.
We mention that

$$\sum_{i=1}^{6}\left(\left(c_i^{(2)}\right)^2 - \frac{|c_i|^2}{2}\right)N_i = -\sum_{i=1}^{6}\left(\left(c_i^{(1)}\right)^2 - \frac{1}{2}\right)N_i = -v. \tag{20}$$

Finally, the third-order moment

$$q = \sum_{i=1}^{6} c_i^{(1)}\left(\left(c_i^{(2)}\right)^2 - \frac{1}{4}\right)N_i \tag{21}$$

is considered; q is the analogue of A and v, w are the analogue of the components of B in Section 2. There is a one-to-one relation between the kinetic variables N_i, $i = 1, \ldots, 6$, and $u_1, u_2, \theta, v, w, q$. All other moments can be written as linear combinations of the above. In particular, we use

$$\begin{aligned}
\sum_{i=1}^{6} \left(c_i^{(1)}\right)^2 N_i &= v + \theta + \frac{C}{2} \\
\sum_{i=1}^{6} \left(c_i^{(2)}\right)^2 N_i &= \theta + \frac{C}{2} - v \\
\sum_{i=1}^{6} \left(c_i^{(1)}\right)^3 N_i &= \frac{3}{4}u_1 - q \\
\sum_{i=1}^{6} \left(c_i^{(2)}\right)^3 N_i &= \frac{3}{4}u_2 \\
\sum_{i=1}^{6} c_i^{(1)} \left(c_i^{(2)}\right)^2 N_i &= \frac{1}{4}u_1 + q \\
\sum_{i=1}^{6} \left(c_i^{(1)}\right)^2 c_i^{(2)} N_i &= \frac{1}{4}u_2 \\
\sum_{i=1}^{6} \left(c_i^{(1)}\right)^2 \left(c_i^{(2)}\right)^2 N_i &= \frac{1}{4}\left(\theta + \frac{C}{2} - v\right) \\
\sum_{i=1}^{6} c_i^{(1)} \left(c_i^{(2)}\right)^3 N_i &= \frac{3}{4}w.
\end{aligned} \tag{22}$$

We proceed further with the diffusion scaling for the discrete velocity model analogous to the continuous case. The diffusion scaling leads to

$$\partial_t N_i + \frac{1}{\epsilon}\partial_x c_i^{(1)} N_i + \frac{1}{\epsilon}\partial_y c_i^{(2)} N_i = \frac{1}{\epsilon^2} J^i(N). \tag{23}$$

The normalized Maxwellian with zero drift, around which we linearize, is in this case simply

$$M_i = \frac{1}{6}. \tag{24}$$

Analogous to Section 2 we use $M_i(1 + \epsilon \tilde{N}_i)$, instead of N_i in the scaled equation (23). Writing again N_i for $\tilde{N}_i$ this leads to

$$\partial_t N_i + \frac{1}{\epsilon}\partial_x c_i^{(1)} N_i + \frac{1}{\epsilon}\partial_y c_i^{(2)} N_i = \frac{1}{\epsilon^2} J^i(N) \tag{25}$$

with

$$J^i(N) = L^i(N) + \epsilon Q_i(N, N), \tag{26}$$

where

$$L^i(N) = -\frac{1}{\tau}\left(N_i - N_i^{leq}\right) \tag{27}$$

with the linearized equilibrium distribution

$$N_i^{leq} = \frac{\rho}{6} + \frac{1}{3}\left(c_i^{(1)}u_1 + c_i^{(2)}u_2\right) \tag{28}$$

and

$$Q_i(N,N) = \frac{2}{3\tau}\sum_{k,l}\left(c_i^{(k)}c_i^{(l)} - \frac{1}{2}\delta_{k,l}\right)u_k u_l. \tag{29}$$

One observes that for $\epsilon \to 0$ $N_i \to N_i^{leq}$ and thus $v, w, q \to 0$ as $\epsilon \to 0$. Moreover, since $\partial_x \sum (c_i^{(1)})^2 N_i^{leq}$ and $\partial_y \sum (c_i^{(2)})^2 N_i^{leq}$ tend to 0 as $\epsilon \to 0$, we get that $\partial_x \rho$ and $\partial_y \rho$ tend to 0. Thus, ρ is constant in space and time as $\epsilon \to 0$, if suitable boundary conditions are imposed.

To obtain the scaled moment equations we use $u_1, u_2, p = \theta - |u|^2/2$ as before, with the scaled quantities

$$\theta = \frac{1}{\epsilon}\frac{1}{2}\left(\sum_{i=1}^{6} N_i - C\right) \tag{30}$$

and

$$\begin{aligned} v &= \frac{1}{\epsilon}\sum_{i=1}^{6}\left(\left(c_i^{(1)}\right)^2 - \frac{1}{2}\right)N_i \\ w &= \frac{1}{\epsilon}\sum_{i=1}^{6} c_i^{(1)}c_i^{(2)}N_i \end{aligned} \tag{31}$$

$$q = \frac{1}{\epsilon^2}\sum_{i=1}^{6} c_i^{(1)}\left(\left(c_i^{(2)}\right)^2 - \frac{1}{4}\right)N_i. \tag{32}$$

The scaling corresponds to the fact that the above-mentioned quantities tend to 0 as $\epsilon \to 0$. The constant C is defined such that $\sum N_i = \rho$ tends to C as ϵ tends to 0 (ρ approaches a constant due to the above).

Multiplication of (25) with $c_i^{(1)}$, $c_i^{(2)}$, $|c_i|^2/2$, $(c_i^{(1)})^2 - \frac{1}{2}$, $c_i^{(1)}c_i^{(2)}$, $c_i^{(1)}((c_i^{(2)})^2 - \frac{1}{4})$ and summation over i gives (using (22)) the closed system of moment equations for the macroscopic variables:

$$\begin{aligned} \partial_t u_1 + \partial_x v + \partial_y w + \partial_x \theta &= 0 \\ \partial_t u_2 + \partial_x w - \partial_y v + \partial_y \theta &= 0 \\ \partial_t \theta + \frac{1}{\epsilon^2}\left(\partial_x\left(\frac{1}{2}u_1\right) + \partial_y\left(\frac{1}{2}u_2\right)\right) &= 0 \end{aligned} \tag{33}$$

$$\begin{aligned} \partial_t v + \frac{1}{\epsilon^2}\left(\partial_x\left(\frac{1}{4}u_1 - \epsilon^2 q\right) - \partial_y\left(\frac{1}{4}u_2\right)\right) &= -\frac{1}{\epsilon^2\tau}\left(v - \frac{1}{2}(u_1^2 - u_2^2)\right) \\ \partial_t w + \frac{1}{\epsilon^2}\left(\partial_x\left(\frac{1}{4}u_2\right) + \partial_y\left(\frac{1}{4}u_1 + \epsilon^2 q\right)\right) &= -\frac{1}{\epsilon^2\tau}(w - u_1 u_2) \\ \partial_t q + \frac{1}{\epsilon^2}\left(-\partial_x\left(\frac{1}{2}v\right) + \partial_y\left(\frac{1}{2}w\right)\right) &= -\frac{1}{\epsilon^2\tau}q. \end{aligned} \tag{34}$$

This is a hyperbolic system with stiff relaxation terms and a partially stiff advection part. Writing the linear main part as

$$\partial_t z + A\partial_x z + B\partial_y z \tag{35}$$

with $z = (u_1, u_2, \theta, v, w, q)$ one observes that the matrix A has three positive and three negative eigenvalues and B has two positive, two negative, and two zero eigenvalues. This gives, in particular, the number of boundary conditions which have to be imposed on the characteristic variables; compare Section 5 for an example. Moreover, initial conditions have to be imposed.

Formally, the diffusion limit of the above system is straightforwardly determined. As $\epsilon \to 0$ the equation for θ reduces to the incompressibility condition:

$$\partial_x u_1 + \partial_y u_2 = 0. \tag{36}$$

The equations for v and w reduce to

$$v = -\partial_x\left(\frac{\tau}{4}u_1\right) + \partial_y\left(\frac{\tau}{4}u_2\right) + \frac{1}{2}\left(u_1^2 - u_2^2\right) \tag{37}$$

and

$$w = -\partial_x\left(\frac{\tau}{4}u_2\right) - \partial_y\left(\frac{\tau}{4}u_1\right) + u_1u_2. \tag{38}$$

This yields

$$\begin{aligned} \partial_t u_1 + \partial_x \frac{1}{2}\left(u_1^2 - u_2^2\right) + \partial_y u_1u_2 + \partial_x\theta &= \frac{\tau}{4}\Delta u_1 \\ \partial_t u_2 + \partial_x u_1u_2 - \partial_y \frac{1}{2}\left(u_1^2 - u_2^2\right) + \partial_y\theta &= \frac{\tau}{4}\Delta u_2, \end{aligned} \tag{39}$$

or using the definition of p,

$$\begin{aligned} \partial_t u_1 + \partial_x\left(u_1^2\right) + \partial_y u_1u_2 + \partial_x p &= \frac{\tau}{4}\Delta u_1 \\ \partial_t u_2 + \partial_x u_1u_2 + \partial_y\left(u_2^2\right) + \partial_y p &= \frac{\tau}{4}\Delta u_2. \end{aligned} \tag{40}$$

These are the Navier–Stokes momentum equations with Reynolds number $\mathrm{Re} = 4/\tau$.

4. THE NUMERICAL SCHEME: TIME DISCRETIZATION

We consider the system of equations

$$\begin{aligned} \partial_t u_1 + \partial_x v + \partial_y w + \partial_x\theta &= 0 \\ \partial_t u_2 + \partial_x w - \partial_y v + \partial_y\theta &= 0 \end{aligned} \tag{41}$$

$$\partial_t\theta + \frac{1}{2\epsilon^2}(\partial_x u_1 + \partial_y u_2) = 0, \tag{42}$$

together with

$$\begin{aligned}\partial_t v &= -\frac{1}{\epsilon^2}\left(\partial_x\left(\frac{1}{4}u_1 - \epsilon^2 q\right) - \partial_y\left(\frac{1}{4}u_2\right) + \frac{1}{\tau}\left(v - \frac{1}{2}\left(u_1^2 - u_2^2\right)\right)\right)\\ \partial_t w &= -\frac{1}{\epsilon^2}\left(\partial_x\left(\frac{1}{4}u_2\right) + \partial_y\left(\frac{1}{4}u_1 + \epsilon^2 q\right) + \frac{1}{\tau}(w - u_1 u_2)\right)\end{aligned} \tag{43}$$

$$\partial_t q = -\frac{1}{\epsilon^2}\left(-\partial_x\left(\frac{1}{2}v\right) + \partial_y\left(\frac{1}{2}w\right) + \frac{1}{\tau}q\right). \tag{44}$$

As ϵ tends to 0 the system becomes stiff. Nevertheless, in lattice–Boltzmann methods a fully explicit discretization is used. We will treat the system by a semi-implicit method. The nonstiff parts are treated explicitly and the stiff ones are treated in an implicit way. In particular, the pressure–velocity coupling is treated in an implicit way. This leads to the usual projection scheme for the incompressible Navier–Stokes equations in the small mean free path limit $\epsilon \to 0$.

The time discretization of the u_1, u_2, θ equations is given by

$$\begin{aligned}u_1^{k+1} &= u_1^k - \Delta t\left(\partial_x v^k + \partial_y w^k + \partial_x \theta^{k+1}\right)\\ u_2^{k+1} &= u_2^k - \Delta t\left(\partial_x w^k - \partial_y v^k + \partial_y \theta^{k+1}\right)\end{aligned} \tag{45}$$

$$\theta^{k+1} = \theta^k - \frac{\Delta t}{\epsilon^2}\left(\partial_x u_1^{k+1} + \partial_y u_2^{k+1}\right). \tag{46}$$

Using Eqs. (45) in Eq. (46) yields a Helmholtz equation for the pressure:

$$\Delta_{x,y}\theta^{k+1} - \frac{\epsilon^2}{\Delta t^2}\theta^{k+1} = \frac{1}{\Delta t}\left(\partial_x u_1^k + \partial_y u_2^k\right) - \left(\partial_x^2 v^k + 2\partial_x\partial_y w^k - \partial_y^2 v^k\right) - \frac{\epsilon^2}{\Delta t^2}\theta^k. \tag{47}$$

Boundary conditions for the Helmholtz equation are determined from Eq. (41) and the conditions imposed on the hyperbolic system (see the last section for an example). This equation is solved by an iterative procedure; u_1, u_2 are then determined from Eq. (45).

The remaining equations are treated as

$$\begin{aligned}v^{k+1} = v^k - \frac{\Delta t}{\epsilon^2}\Bigg(&\partial_x\left(\frac{1}{4}u_1^{k+1} - \epsilon^2 q^k\right) - \partial_y\left(\frac{1}{4}u_2^{k+1}\right)\\ &+ \frac{1}{\tau}\left(v^{k+1} - \frac{1}{2}\left(\left(u_1^{k+1}\right)^2 - \left(u_2^{k+1}\right)^2\right)\right)\Bigg),\end{aligned} \tag{48}$$

$$w^{k+1} = w^k - \frac{\Delta t}{\epsilon^2}\left(\partial_x\left(\frac{1}{4}u_2^{k+1}\right) + \partial_y\left(\frac{1}{4}u_1^{k+1} + \epsilon^2 q^k\right) + \frac{1}{\tau}\left(w^{k+1} - u_1^{k+1}u_2^{k+1}\right)\right), \tag{49}$$

$$q^{k+1} = q^k - \frac{\Delta t}{\epsilon^2}\left(-\partial_x\left(\frac{1}{2}v^{k+1}\right) + \partial_y\left(\frac{1}{2}w^{k+1}\right) + \frac{1}{\tau}q^{k+1}\right). \tag{50}$$

Introducing

$$\lambda(\epsilon) = \frac{\Delta t}{\tau\epsilon^2}\left(1 + \frac{\Delta t}{\tau\epsilon^2}\right)^{-1},$$

we get

$$
\begin{aligned}
v^{k+1} &= \frac{\epsilon^2\tau}{\Delta t}\lambda v^k - \lambda\tau\left(\partial_x\left(\frac{1}{4}u_1^{k+1} - \epsilon^2 q^k\right) - \partial_y\left(\frac{1}{4}u_2^{k+1}\right) - \frac{1}{\tau 2}\left(\left(u_1^{k+1}\right)^2 - \left(u_2^{k+1}\right)^2\right)\right),\\
w^{k+1} &= \frac{\epsilon^2\tau}{\Delta t}\lambda w^k - \lambda\tau\left(\partial_x\left(\frac{1}{4}u_2^{k+1}\right) + \partial_y\left(\frac{1}{4}u_1^{k+1} + \epsilon^2 q^k\right) - \frac{1}{\tau}u_1^{k+1}u_2^{k+1}\right),\\
q^{k+1} &= \frac{\epsilon^2}{\Delta t}\lambda q^k - \lambda\tau\left(-\partial_x\left(\frac{1}{2}v^{k+1}\right) + \partial_y\left(\frac{1}{2}w^{k+1}\right)\right).
\end{aligned}
\tag{51}
$$

5. THE INCOMPRESSIBLE NAVIER–STOKES LIMIT

Obviously, the time discretized scheme tends to a time discretization of the incompressible Navier–Stokes equations. We obtain as before

$$
\begin{aligned}
u_1^{k+1} &= u_1^k - \Delta t\left(\partial_x v^k + \partial_y w^k + \partial_x\theta^{k+1}\right),\\
u_2^{k+1} &= u_2^k - \Delta t\left(\partial_x w^k - \partial_y v^k + \partial_y\theta^{k+1}\right).
\end{aligned}
\tag{52}
$$

Moreover, one obtains the usual Poisson equation for the pressure:

$$
\Delta_{x,y}\theta^{k+1} = \frac{1}{\Delta t}\left(\partial_x u_1^k + \partial_y u_2^k\right) - \left(\partial_x^2 v^k + 2\partial_x\partial_y w^k - \partial_y^2 v^k\right). \tag{53}
$$

This yields, if combined with (52) the incompressibility constraint,

$$
\partial_x u_1^{k+1} + \partial_y u_2^{k+1} = 0.
$$

Noting that λ tends to 1 as ϵ tends to 0, we get

$$
\begin{aligned}
v^{k+1} &= -\left(\partial_x\left(\frac{\tau}{4}u_1^{k+1}\right) - \partial_y\left(\frac{\tau}{4}u_2^{k+1}\right) - \frac{1}{2}\left(\left(u_1^{k+1}\right)^2 - \left(u_2^{k+1}\right)^2\right)\right),\\
w^{k+1} &= -\left(\partial_x\left(\frac{\tau}{4}u_2^{k+1}\right) + \partial_y\left(\frac{\tau}{4}u_1^{k+1}\right) - u_1^{k+1}u_2^{k+1}\right),\\
q^{k+1} &= -\partial_x\left(\frac{\tau}{2}v^{k+1}\right) + \partial_y\left(\frac{\tau}{2}w^{k+1}\right).
\end{aligned}
\tag{54}
$$

One obtains the usual projection method for the incompressible Navier–Stokes equations (40) (see, e.g., [18]).

6. THE NUMERICAL METHOD: SPACE DISCRETIZATION

As mentioned in the Introduction any grid could be used to solve the discrete velocity model. Thus, we do not use a hexagonal grid as in the lattice–Boltzmann method. Instead, the space discretization is done using a staggered grid as in the MAC method with

$$
x_{\gamma,\delta} = (\gamma h, \delta h),
$$

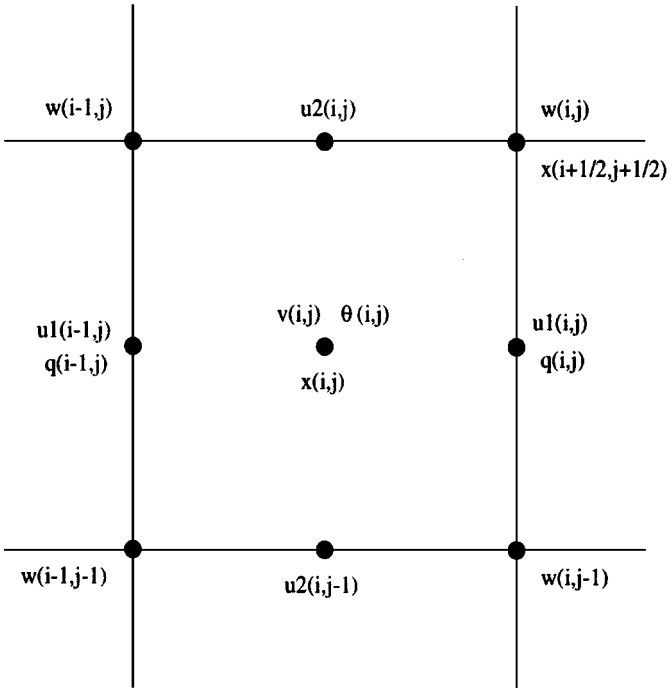

FIG. 1. Grid.

where γ, δ are integer or half integer values. Considering a control volume with edges $x_{i-1/2,j-1/2}$, where i, j are integer values, the quantities $u_1, u_2, \theta, v, w, q$ are evaluated at the following points (see Fig. 1); v and θ are evaluated at the center of the controlvolumes, w at the gridpoints; u_1 and q are evaluated at the west and east faces and u_2 is evaluated at the north and south faces of the control volumes. That means we consider v and θ at $x_{i,j}$, u_1, q at $x_{i-1/2,j}$, u_2 at $x_{i,j-1/2}$, and w at $x_{i-1/2,j-1/2}$.

The derivatives are all determined using centered differences. In order to solve the equations we need to determine u_1, u_2 at $x_{i,j}$ and at $x_{i-1/2,j-1/2}$. This is simply done using linear interpolation; for example, $(u_1)_{i,j} = \frac{1}{2}((u_1)_{i-1/2,j} + (u_1)_{i+1/2,j})$. Thus, no upwinding is included here.

Boundary conditions are treated in the usual way by linear interpolation at the boundaries for those values which are not located on the boundaries.

7. NUMERICAL RESULTS AND EXAMPLES

We consider a driven cavity situation with $(x, y) \in [0, 1]^2$. The usual boundary conditions in this situation for the continuous kinetic equation are diffuse reflection. That means, that R^x in Section 2, Eq. (3), is given by

$$R^x(v, v') = \frac{1}{M}|v \cdot n|\left(1 + v \cdot n^{\perp}\frac{\bar{u}}{\bar{\rho}}\right), \tag{55}$$

where $n^{\perp}$ denotes the vector tangential to the boundary, $\bar{u}/\bar{\rho}$ is the drift in this direction, and $\bar{M}$ is defined by

$$\bar{M} = \int_{v' \cdot n < 0} |v' \cdot n| M(v')\, dv'$$

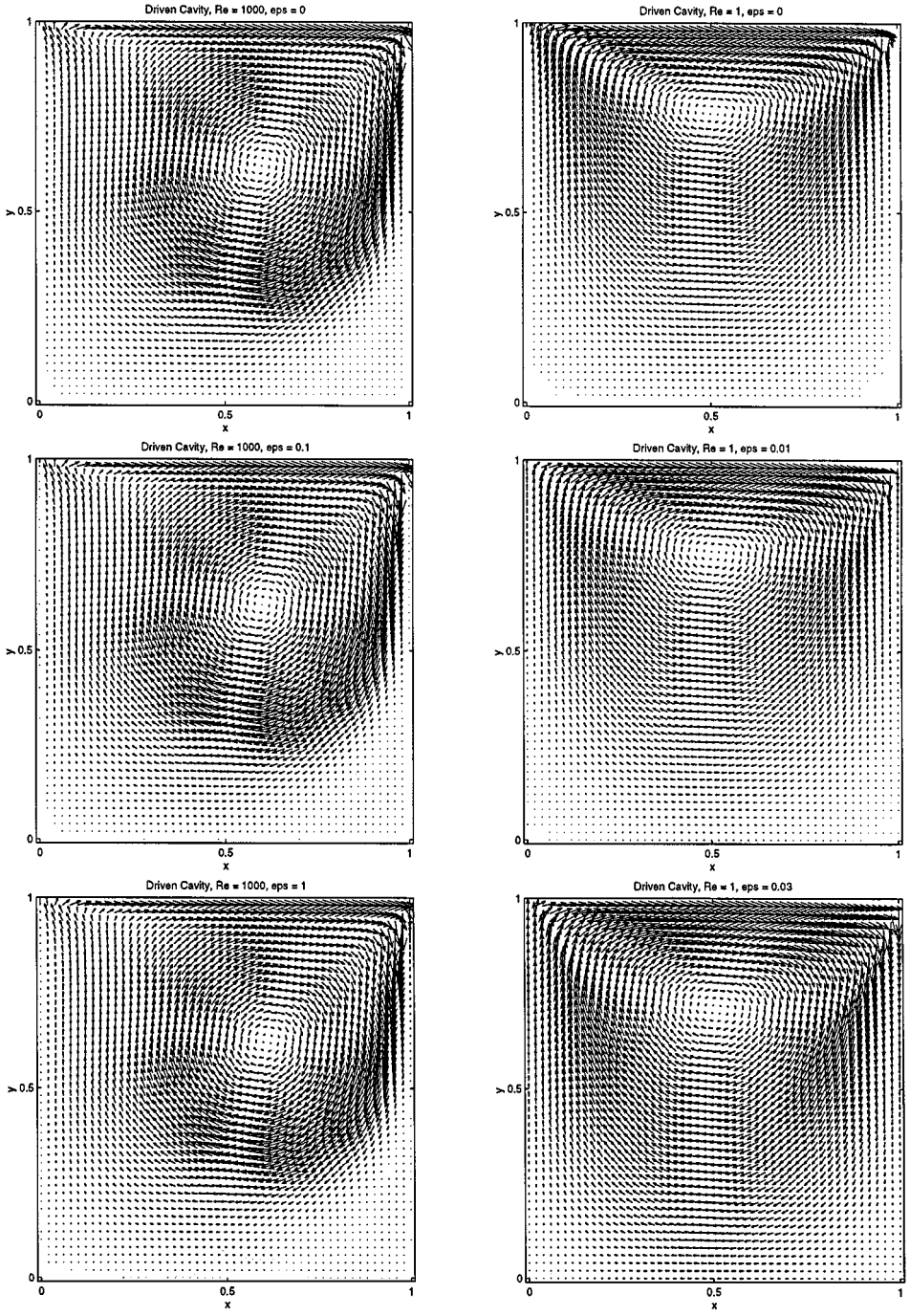

FIG. 2. Driven cavity; vector plots of velocities. On the left: $\mathrm{Re} = 1000, \epsilon = 10^{-8}, 0.1, 1$; on the right: $\mathrm{Re} = 1, \epsilon = 10^{-8}, 0.01, 0.03$.

in order to fulfill (8). This means we assume complete accomodation with a drift $\bar{u}/\bar{\rho}$ parallel to the boundary. At the top of the square $\bar{u} > 0$ and $\bar{u} = 0$ at the other three sides.

The boundary conditions for the hyperbolic system (33, 34) are derived from the kinetic formulation (25) and then rewritten in terms of the macroscopic variables. In terms of the

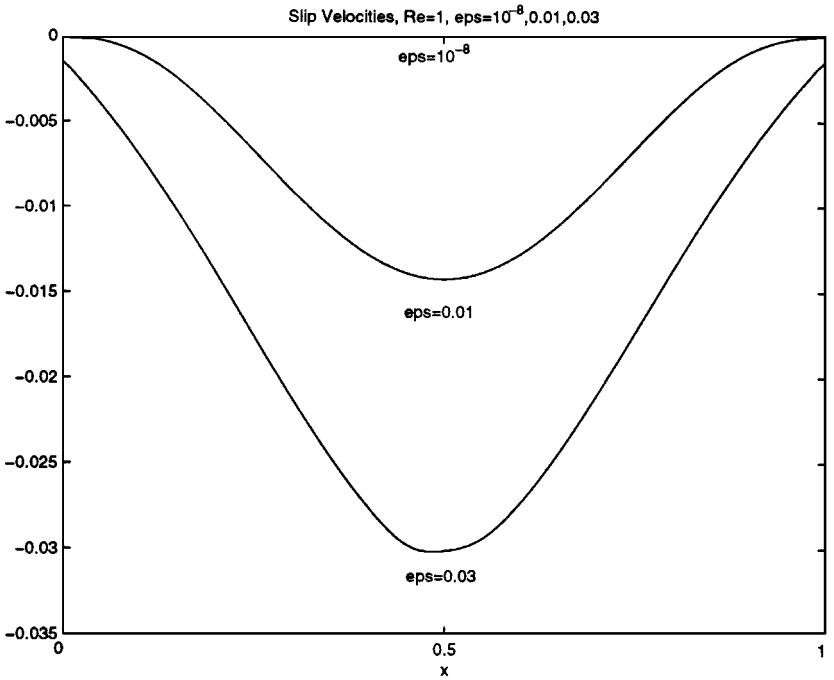

FIG. 3. Slip velocities for $\mathrm{Re} = 1$ and different values of ϵ.

discrete kinetic variables N_i the boundary conditions corresponding to diffuse reflection are:

On the west face N_i, $i = 1, 2, 6$, are given by α, where α is found by (compare Eq. (9))

$$\sum_{i=3,4,5} \left|c_i^{(1)}\right| N_i M_i = \alpha \sum_{i=1,2,6} \left|c_i^{(1)}\right| M_i.$$

This corresponds to (7) combined with (55) with $\bar{u} = 0$. M_i is given by (24). This yields

$$N_i = \frac{1}{4}(N_3 + 2N_4 + N_5), \quad i = 1, 2, 6.$$

In terms of the macroscopic variables this leads to

$$u_1 = 0$$
$$u_2 = 2\epsilon w$$
$$3v = 8\epsilon q.$$

On the north face N_5, N_6 are given by $N_i = \alpha M_i^{\bar{u}} M_i^{-1}$, $i = 5, 6$, where α is given by (compare again (9))

$$\sum_{i=2,3} \left|c_i^{(2)}\right| N_i M_i = \alpha \sum_{i=5,6} \left|c_i^{(2)}\right| M_i.$$

$M_i^{\bar{u}}$ is, again analogous to (7), combined with (55), given by $(1 + 2c_i^{(1)}\bar{u}/\bar{\rho})M_i$. We use

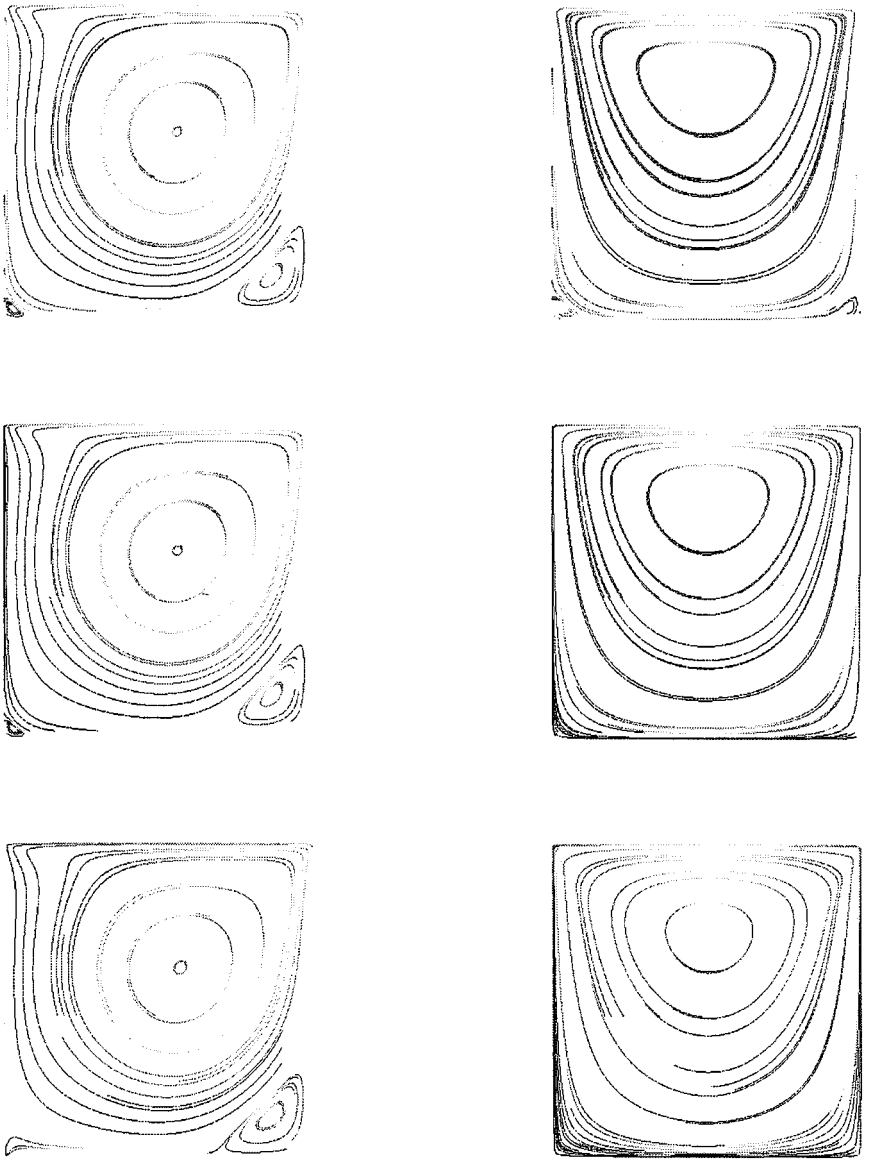

FIG. 4. Driven cavity; streamlines. On the left, from above: $\mathrm{Re} = 1000$, $\epsilon = 10^{-8}$, 0.1, 1; on the right, from above: $\mathrm{Re} = 1$, $\epsilon = 10^{-8}$, 0.01, 0.03.

$\bar{\rho} = 1$. Thus, the constant C used in Section 3 is given by 1. We obtain

$$N_5 = \frac{1}{2}(N_2 + N_3)(1 - \bar{u})$$

$$N_6 = \frac{1}{2}(N_2 + N_3)(1 + \bar{u}).$$

In terms of the macroscopic variables this is

$$u_1 = \bar{u} + \epsilon\bar{u}(2\theta - 2v) + \epsilon(2\sqrt{3}w - 8\epsilon q)$$

$$u_2 = 0.$$

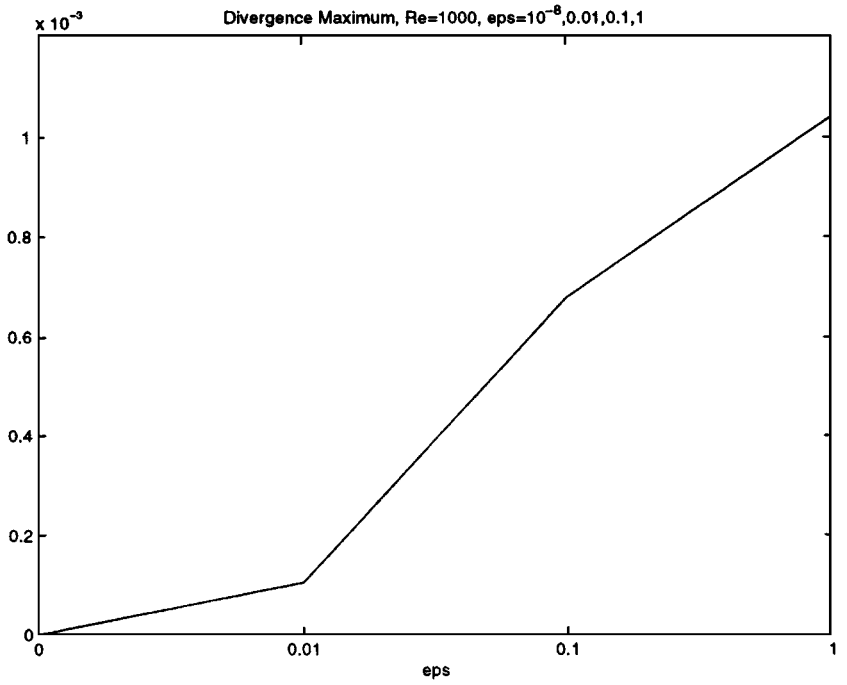

FIG. 5. Divergence maximum for different values of ϵ and $\mathrm{Re} = 1000$.

We have three and two conditions, respectively, fitting to the required numbers of boundary conditions for the hyperbolic system (see Section 3). East and south faces are treated in an analogous way. The boundary conditions for the Helmholtz equation are due to $u_1 n_1 + u_2 n_2 = 0$, where $n = (n_1, n_2)$ is again the normal to the boundary, and (45) is found by

$$n_1 \partial_x \theta + n_2 \partial_y \theta = -n_1(\partial_x v + \partial_y w) - n_2(\partial_x w - \partial_y v).$$

For the simulation zero initial conditions are used for u, θ, v, w, q; $\bar{u}$ is chosen equal to 1. Figure 2 shows vector plots of the velocities for $\mathrm{Re} = 1000$ and $\epsilon = 10^{-8}$, $\epsilon = 0.1$, $\epsilon = 1$ at time $T = 15$, and for $\mathrm{Re} = 1$ and $\epsilon = 10^{-8}$, $\epsilon = 0.01$, $\epsilon = 0.03$ at $T = 1$, respectively. In particular, for $\mathrm{Re} = 1$ the kinetic velocity slip is observed at the boundaries for a larger Knudsen number ϵ.

In Fig. 3 plots of the slip velocities for different values of the Knudsen number ϵ are shown. The figure shows the slip velocities along a horizontal section at the bottom of the box for $\mathrm{Re} = 1$ at time $T = 1$. For $\epsilon = 10^{-8}$ the slip velocities are zero.

In Fig. 4 streamline plots of the same situations as in Fig. 2 are shown. In particular, for $\mathrm{Re} = 1000$ the vortices at the lower edges are observed.

Finally, in Fig. 5 the divergence maximum at time $T = 0.01$ for different values of the Knudsen number ϵ is shown for $\mathrm{Re} = 1000$.

8. CONCLUSIONS

• Considering a lattice Boltzmann type discrete velocity model, a numerical scheme working uniformly in the incompressible Navier Stokes limit has been presented.

- The above kinetic model is simple. However, physically more relevant microscopic systems could be studied as well and treated in a similar way.
- The scheme is based is semiimplicit discretization preserving the asymptotic limit. For small ϵ the scheme tends to a standard projection scheme for the imcompressible Navier Stokes equations. For $\epsilon > 0$ in contrast to the projection method a Helmholtz equation instead of the usual Poisson equation has to be solved.
- In further work an upwinding procedure should be included in the method. This may lead to other discretizations for the limit Navier Stokes equations.
- Moreover, connections to the relaxation schemes presented in [13, 12] should be explored. See also [5].
- The procedures described in the paper are formal. Rigorous mathematical results should be considered in further work. See, for example [4, 16] for rigorous work in related fields.

ACKNOWLEDGMENTS

Useful discussions with M. Günther, G. Gramlich, M. Junk, and J. Struckmeier are gratefully acknowledged.

REFERENCES

1. T. Abe, Derivation of the lattice Boltzmann method by means of the discrete ordinate method for the Boltzmann equation, *J. Comput. Phys.* **131**, 241 (1997).
2. C. Bardos, F. Golse, and D. Levermore, Fluid dynamic limits of kinetic equations: Formal derivations, *J. Stat. Phys.* **63**, 323 (1991).
3. S. Benzi, R. Succi, and M. Vergassola, The lattice–Boltzmann equation: Theory and applications, *Phys. Rep.* **222**, 145 (1992).
4. R. E. Caflisch, S. Jin, and G. Russo, Uniformly accurate schemes for hyperbolic systems with relaxation, *SIAM J. Num. Anal.* **34**, 246 (1997).
5. N. Cao, S. Chen, S. Jin, and D. Martinez, Physical symmetry and lattice symmetry in lattice Boltzmann methods, *Phys. Rev. E* **55**, 21 (1997).
6. C. Cercignani, *The Boltzmann Equation and Its Applications* (Springer-Verlag, New York/Berlin, 1988).
7. H. Chen, S. Chen, and W. Matthaeus, Recovery of the Navier–Stokes equations using a lattice-gas Boltzmann method, *Phys. Rev. A* **45**, 5339 (1992).
8. A. J. Chorin, Numerical solution of the Navier–Stokes equations, *Math. Comp.* **22**, 745 (1968).
9. A. De Masi, R. Esposito, and J. L. Lebowitz, Incompressible Navier Stokes and Euler limits of the Boltzmann equation, *Comm. Pure Appl. Math.* **42**, 1189 (1989).
10. U. Frisch, D. d'Humieres, B. Hasslacher, P. Lallemand, Y. Pomeau, and J. P. Rivet, Lattice gas hydrodynamics in two and three dimensions, *Complex Systems* **1**, 649 (1987).
11. S. Jin and D. Levermore, Numerical schemes for hyperbolic conservation laws with stiff relaxation terms, *J. Comput. Phys.* **126**, 449 (1996).
12. S. Jin, L. Pareschi, and G. Toscani, Diffusive relaxation schemes for discrete-velocity kinetic equations, *SIAM J. Num. Anal.* **35**, 2405 (1998).
13. S. Jin and Z. Xin, The relaxation schemes for systems of conservation laws in arbitrary space dimensions, *Comm. Pure Appl. Math.* **48**, 235 (1995).
14. M. Junk, Kinetic schemes in lattice Boltzmann form, preprint.
15. A. Klar, A numerical method for kinetic semiconductor equations in the drift diffusion limit, *SIAM J. Sci. Comp.*, to appear.
16. A. Klar, An asymptotic-induced scheme for nonstationary transport equations in the diffusive limit, *SIAM J. Num. Anal.* **35**, 1073 (1997).

17. E. W. Larsen and J. E. Morel, Asymptotic solution of numerical transport problems in optically thick, diffusive regimes II, *J. Comput. Phys.* **83**, **212** (1989).
18. R. Peyret and T. Taylor, *Computational Methods for Fluid Flow*, Series in Computational Fluids (Springer-Verlag, Berlin, 1983).
19. T. Platkowski and R. Illner, Discrete velocity models of the Boltzmann equations, *SIAM Rev.* **30**, 213 (1988).
20. J. Sterling and S. Chen, Stability analysis of lattice Boltzmann methods, *J. Comput. Phys.* **123**, 196 (1996).
21. B. Wetton, Analysis of the spatial error for a class of finite difference methods for viscous incompressible flow, *SIAM J. Num. Anal.* **34**, 723 (1997).